Letter

Influence of topological degeneracy on the boundary Berezinskii-Kosterlitz-Thouless quantum phase transition of a dissipative resonant level

Gu Zhang [1,*] Zhan Cao [1] and Dong E. Liu [2,1,3,4,†]

[1] Beijing Academy of Quantum Information Sciences, Beijing 100193, China
[2] State Key Laboratory of Low Dimensional Quantum Physics, Department of Physics, Tsinghua University, Beijing 100084, China
[3] Frontier Science Center for Quantum Information, Beijing 100184, China
[4] Hefei National Laboratory, Hefei 230088, China

(Received 20 March 2023; revised 25 March 2024; accepted 1 April 2024; published 17 April 2024)

The interplay between a topological degeneracy and the residue degeneracy (also known as the residue entropy) of quantum criticality remains an important but not thoroughly understood topic. We find that this topological degeneracy, provided by a Majorana zero mode pair, relaxes the otherwise strictly requested symmetry requirement, to observe the boundary Berezinskii-Kosterlitz-Thouless (BKT) quantum phase transition (QPT) of a dissipative resonant level. Our work indicates that the topological degeneracy can be potentially viewed as an auxiliary symmetry that realizes a robust boundary QPT. The relaxation of the symmetry requirement extends the transition from a point to a finite area, thus greatly reducing the difficulty to experimentally observe the QPT. This topology-involved exotic BKT phase diagram, on the other hand, provides another piece of evidence that can further confirm the existence of a Majorana zero mode.

DOI: 10.1103/PhysRevB.109.L161110

Introduction. Boundary quantum phase transitions (QPTs) [1,2] are special QPTs triggered by the change of boundary conditions. Similar to the bulk ones, boundary QPTs normally involve symmetries. For instance, in multichannel Kondo [3–7], Luttinger liquid resonant [8], multiple-impurity Anderson or Kondo [9–15], and dissipative resonant level [16–18] models, the observation of quantum critical point (QCP) requires the impurity to symmetrically couple to involved leads. Actually, the symmetric coupling that triggers quantum frustration at QCP produces a nontrivial residue degeneracy, which is another important feature of QPT [1,3]. This residue degeneracy, heavily focused on recently as a QPT-induced "anyon" [7,19–22], has been proposed as an amplifier of topological nontriviality [23]. As another example, a Berezinskii-Kosterlitz-Thouless (BKT) transition is predicted in a dissipative resonant level model (DRLM) [18,24] between the ballistic-transmission and isolated-impurity phases. Its observation, importantly, also requires perfectly symmetric lead-dot couplings [18,24]. This fine-tuning prerequisite of symmetry is among the difficulties to observe this BKT QPT. To the best of our knowledge, a BKT-type boundary QPT has not yet been reported experimentally.

On the other hand, a pair of Majorana zero modes (MZMs), predicted to exist at end points of a nanowire heterostructure [25–27] and vortices of a topological superconductor [28,29], is known to provide a nonlocally defined topological degeneracy, given a long-enough inter-MZM distance. In addition, the coupling between a topological degeneracy and a lead always has equal electron (i.e., normal tunneling) and hole (i.e., Andreev reflection) components. These two robust features of a topological degeneracy, distinct from a trivially local one, are among the key elements of topological quantum computation [30]. Exploring the intricate influences of topological degeneracy on the residue degeneracy in QPTs, where symmetry is a prerequisite, constitutes a compelling avenue of investigation. A crucial line of inquiry involves investigating the potential role of topological degeneracy as an auxiliary symmetry capable of reinstating boundary QPTs that have been undermined by asymmetry.

In this work, we thus investigate the influence of topological degeneracy on the boundary BKT QPT in a DRLM. Without the topological degeneracy, it is known that the BKT transition of a DRLM requires a perfect symmetry between two involved leads. Surprisingly, as among our central results, this strict symmetry requirement (to observe the BKT QPT) is remarkably relaxed, by coupling an MZM to the dot of the DRLM [see Fig. 2, which is distinct from Fig. 1(b)]. With Coulomb gas renormalization group (RG) equations and g-theorem [31–33], we further prove that the relaxation of symmetry requirement is a direct consequence of the topological degeneracy, with which the left-right asymmetry becomes irrelevant near the strong-tunneling fixed point. Our work, as far as we know, is pioneering in studying the interplay between topological degeneracy and boundary QPTs where symmetries are otherwise strictly requested. In addition, the broadened ballistic-transmission phase space (Fig. 2) greatly reduces the experimental difficulty to observe the BKT QPT of a DRLM. Remarkably, the phase diagram featuring MZMs, which greatly contrasts that of a regular DRLM, provides a clear and unequivocal indicator for detecting the presence of MZMs. In real experiments, to observe our

*zhanggu@baqis.ac.cn
†dongeliu@mail.tsinghua.edu.cn

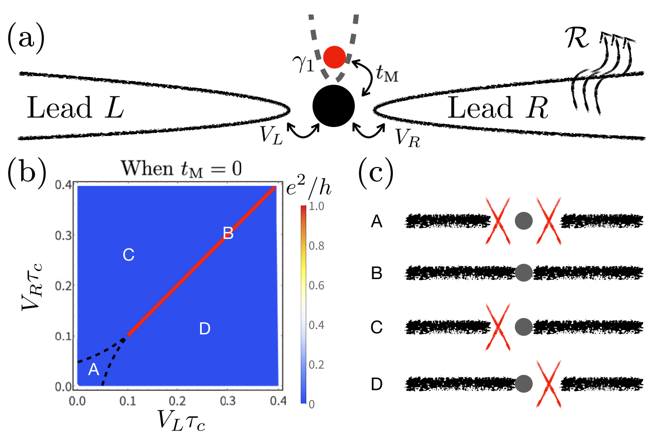

FIG. 1. (a) The model of the system. The MZM (red dot) couples to the dot of the DRLM, with the amplitude t_{M}. The dot couples to two leads with corresponding amplitudes V_L and V_R. The leads are dissipative with the total impedance $\mathcal{R}$. When $t_{\mathrm{M}} = 0$, the system reduces to the DRLM, with the zero-temperature equilibrium conductance in (b) (when $r = 2.5$), as a function of dimensionless quantities $V_L\tau_c$ and $V_R\tau_c$. Here, τ_c is the cutoff in imaginary time. In real systems, $\tau_c \sim 1/D$, with D the relevant bandwidth [34]. In (b), the conductance is determined by the fixed points [with four candidates in (c)] to which the system approaches [figured out by RG equations (2) and (3)] at zero temperature. The marked-out phases A–D are illustrated in (c), with red crosses indicating vanishing lead-dot communications. Of phase B, both dot-lead couplings are transparent, leading to a perfect equilibrium conductance e^2/h at zero temperature. Otherwise (phases A, C, and D), the dot decouples with one or both leads. The corresponding zero-temperature equilibrium conductance vanishes.

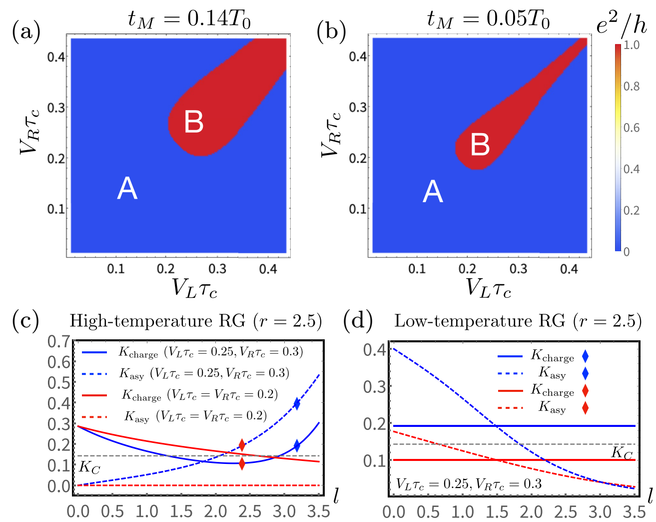

FIG. 2. Phase diagrams (indicated by the corresponding zero-temperature equilibrium conductance) and RG flow curves when $r = 2.5$. (a and b) Phase diagrams with larger ($t_{\mathrm{M}} = 0.14T_0$) and smaller ($t_{\mathrm{M}} = 0.05T_0$) values of t_{M}, respectively. Here, T_0 is the initial temperature of RG flow (i.e., the temperature at which parameters in Hamiltonian are obtained) that requires experimental calibration. Similar to that in Fig. 1(b), the conductance is obtained after identifying the fixed point [A or B, cf. Fig. 1(c)] to which the system flows at zero temperature. (c) High-temperature RG flow curves of K_{charge} and K_{asy}, for the symmetric (red curves) and asymmetric (blue curves) situations. The red and blue diamonds mark points that belong to the ballistic-transmission ($K_{\mathrm{charge}} < K_C$) and isolated-impurity ($K_{\mathrm{charge}} > K_C$) phases, respectively, if high-temperature RG flow terminates at their corresponding l ($l = 0$ when RG initially begins). (d) Low-temperature RG flow of K_{charge} and K_{asy}, with their initial values given by the corresponding diamond.

predicted phenomenon (i.e., phase diagrams in Figs. 1 and 2), the temperature and applied voltage bias are required to be smaller than the Majorana-dot coupling and effective lead-dot hybridizations.

Model. The system we consider [with the Hamiltonian $H = H_{\mathrm{leads}} + H_{\mathrm{impurity}} + H_{\mathrm{T}}$, see Fig. 1(a)] contains two dissipative leads (H_{leads}) that couple to (H_{T}) a Majorana-contained impurity part $H_{\mathrm{impurity}} = \epsilon_d d^\dagger d + it_{\mathrm{M}}(d + d^\dagger)\gamma_1/\sqrt{2}$, where d indicates the dot that couples to one MZM γ_1. The other MZM γ_2 [not shown in Fig. 1(a)] decouples from γ_1, to enforce the exact topological degeneracy. For later convenience, we define an auxiliary fermionic operator $d_{\mathrm{MZM}} \equiv (\gamma_1 - i\gamma_2)/\sqrt{2}$ with MZMs. The lead Hamiltonian H_{leads} contains two free fermionic leads and bosonic environmental modes. With those modes included, the lead-impurity tunneling Hamiltonian $H_{\mathrm{T}} = V_L\psi_L^\dagger de^{i\varphi_L} + V_R\psi_R^\dagger de^{i\varphi_R} + \mathrm{H.c.}$ contains the dynamical phase φ_α that is conjugate to the charge number $N_\alpha = \int dx\psi_\alpha^\dagger(x)\psi_\alpha(x)$, in the corresponding lead $\alpha = L, R$. After integrating out the environmental modes, $\varphi_L = -\varphi_R = \varphi$, with the long-time dynamical feature $\langle\varphi(\tau)\varphi(0)\rangle \sim 2r\ln\tau$ [35], where $r = \mathcal{R}e^2/h$ is the ratio between the Ohmic impedance $\mathcal{R}$ of the dissipative leads, and the resistance quanta h/e^2. The required dissipation has been realized in real experiments [16,17,36,37]. Finally, two leads couple to the dot, with hybridization parameters V_L and V_R.

Dissipative modes introduce an effective many-body interaction to the system [38–40]. We then bosonize lead fermions after extending semi-infinite leads into chiral full-one-dimensional (full-1D) ones [41,42] $\psi_\alpha(x) = F_\alpha \exp[i\phi_\alpha(x)]/\sqrt{2\pi a}$, where a is the short-distance cutoff and F_α is the Klein factor that enforces the fermionic anticommutator. Finally, the bosonic phase ϕ_α satisfies the commutation relation $[\phi_\alpha(x), \phi_{\alpha'}(x')] = i\pi\Theta(x - x')\delta_{\alpha,\alpha'}$. These fields are related to the charge numbers in two leads $N_{L,R} = e[\phi_{L,R}(\infty) - \phi_{L,R}(-\infty)]/(2\pi)$. To proceed, we define the common and difference fields with the rotation $\phi_{c,f} = (\phi_L \pm \phi_R)/\sqrt{2}$. The postrotation fields ϕ_c and ϕ_f reflect the total charge number $N_L + N_R$ and the number difference $N_L - N_R$, respectively. With bosonization and the rotation, the dissipative phase can be combined with the difference field $\phi_f' \equiv (\phi_f + \varphi/\sqrt{2})/\sqrt{1+r}$. The addressed dissipative phase $\varphi' \equiv (\sqrt{r}\phi_f - \varphi/\sqrt{2r})/\sqrt{1+r}$ decouples, reducing the system degrees of freedom.

BKT QPT of the *DRLM*. When the MZM decouples ($t_{\mathrm{M}} = 0$), the system reduces to the regular DRLM, where a boundary BKT QPT is predicted [18] when $2 < r < 3$ and $V_L = V_R$ [43] (see an alternative QPT interpretation in Ref. [24]). When $V_L = V_R$ is larger than a critical value [44], the system flows to the ballistic-transmission phase with conductance e^2/h [line B in the phase diagram of Fig. 1(b)]. Notice that this conductance is different from that of Refs. [45,46], due to the dissipative and interacting effect [16,47–52]. By contrast, with couplings smaller than the critical value, the system instead flows to the isolated-impurity phase [A of Fig. 1(b)] with zero conductance. The transition (between phases A and B) is of BKT type, due to the absence of QCP. Indeed, it shares equivalent scaling equations with those of an XY model, the pioneering model of topological transition [53–55]. More specifically, when $r > 2$, the lead-dot coupling is originally RG irrelevant [i.e., with scaling dimension larger than 1 [56], see Eq. (2)]. The couplings then initially decrease during the RG flow. If $V_L = V_R$ are initially large enough, the dot charge number gradually becomes fixed at half-filling [18,41]. The common field, reflecting the charge number fluctuation, then loses its scaling dimension after the RG, leading to a relevant lead-dot coupling if $r < 3$. Briefly, the change of scaling dimension (upon the RG flow) leads to the BKT QPT: the system can enter the ballistic-transmission phase only if V_L and V_R become relevant before they vanish; otherwise, the flow terminates in the isolated-impurity phase.

Importantly, this BKT QPT requires a strict left-right symmetry $V_L = V_R$. Indeed, if $V_L \neq V_R$, the system flows to other two zero-conductance phases [C and D of Fig. 1(b)]. The transition C $\leftrightarrow$ B $\leftrightarrow$ D, with state B as the QCP, is not of BKT type. As our main result, we show that with a finite Majorana-dot coupling $t_{\rm M}$, the strict left-right symmetry to observe the BKT QPT is relaxed. Indeed, as shown in Fig. 2, the ballistic-transmission phase (area B) has extended from a 1D line [Fig. 1(b)] to a two-dimensional (2D) space. The specific phase diagram changes under the different values of $t_{\rm M}$: when $t_{\rm M}$ decreases [i.e., increasing cutoff l_C, from Fig. 2(a) to Fig. 2(b)], the ballistic-transmission phase requires smaller lead-dot tunnelings, but has a worse tolerance against left-right asymmetry.

Coulomb gas RG. In this work, we obtain the phase diagram of Figs. 2(a) and 2(b) with the method of Coulomb gas RG [41,57]. Briefly, within the Coulomb gas representation, one works with the partition function

$$\mathcal{Z} = \sum_n \int_0^{1/T} d\tau_1 \dots \int_0^{\tau_i-\tau_c} d\tau_{i+1} \dots \int_0^{\tau_{n-1}-\tau_c} d\tau_n \times \langle H_{\rm T}(\tau_1)\dots H_{\rm T}(\tau_{i+1})\dots H_{\rm T}(\tau_n)\rangle_{H_{\rm leads}+H_{\rm impurity}}, \quad (1)$$

where n refers to the number of lead-impurity tunneling events during imaginary time $1/T$, and τ_c is the cutoff: for any $i \in [1, n-1]$, $\tau_i - \tau_{i+1} > \tau_c$ is enforced. Expansions of Eq. (1) are carried out within the interaction picture [58], over lead-impurity tunnelings $H_{\rm T}$. One can perform RG calculations [41] as follows. During each RG step, one starts with the cutoff τ_c and increases it to $\tau_c + d\tau_c$ (indicating the temperature decreasing). The pairs of tunneling events at $\{\tau_i, \tau_{i+1}\}$ with condition $\tau_c < |\tau_i - \tau_{i+1}| < \tau_c + d\tau_c$ should be integrated out. RG flow equations are then obtained, after rescaling the cutoff and enforcing the invariance of $\mathcal{Z}$. In Eq. (1), the correlator of $H_{\rm T}$ equals the product of the free-lead correlation (with the environmental modes included) and the impurity correlation. The free-lead contribution can be straightforwardly obtained [18,41].

The impurity correlator can be obtained by solving the Hamiltonian $H_{\rm impurity}$, leading to four impurity eigenstates: two even-parity ones $|\psi_{1,3}\rangle = \frac{1}{\sqrt{2}}(\mp i|1,1\rangle + |0,0\rangle)$ and two odd-parity ones $|\psi_{2,4}\rangle = \frac{1}{\sqrt{2}}(\mp i|1,0\rangle + |0,1\rangle)$, where $|n,m\rangle$ indicates the state with n and m particle (either 0 or 1) in the dot and the auxiliary dot $d_{\rm MZM}$, respectively. Assuming $t_{\rm M} > 0$, states $|\psi_1\rangle$ and $|\psi_2\rangle$ become the degenerate ground states: they have the energy $-t_{\rm M}$, lower than that ($t_{\rm M}$) of $|\psi_3\rangle$ and $|\psi_4\rangle$.

Without lead-dot tunneling, the impurity part stays in two possible ground states, $|\psi_1\rangle$ and $|\psi_2\rangle$. This double-degeneracy originates from the topological degeneracy. After one lead-dot tunneling, they become $d|\psi_1\rangle = -\frac{i}{2}(|\psi_2\rangle + |\psi_4\rangle)$, $d^\dagger|\psi_1\rangle = \frac{i}{2}(|\psi_2\rangle - |\psi_4\rangle)$, $d|\psi_2\rangle = -\frac{i}{2}(|\psi_1\rangle + |\psi_3\rangle)$, and $d^\dagger|\psi_2\rangle = \frac{i}{2}(|\psi_1\rangle - |\psi_3\rangle)$, resulting in (noneigen) final states with impurity parities different from the initial ones. The impurity state before the next lead-impurity tunneling depends on the evolution time [44]. For the low-temperature limit $T \ll t_{\rm M}$, tunnelings are rare; the impurity state evolves back to the ground states $|\psi_1\rangle$ and $|\psi_2\rangle$ before the next tunneling. By contrast, for the high-temperature situation $T \gg t_{\rm M}$, lead-dot tunnelings are frequent, and the impurity state stays in the noneigenstate before the next lead-impurity tunneling. We thus have to treat the low-temperature and high-temperature situations separately.

The high-temperature RG flow. We start by visiting the high-temperature regime $T \gg t_{\rm M}$, where all four impurity states are energetically allowed. Of this case, the impurity-lead tunneling histories with alternating creation and annihilation operators dominate the partition function [44]. The effect of the MZM-dot coupling is then negligible, leading to RG equations that approximately equal that of a normal DRLM (following Ref. [18], or reducing Luttinger liquid spinful results of Ref. [34] to the spinless case),

$$\begin{aligned} dV_{L,R}/dl &= V_{L,R}\left[1 - \frac{1+r}{4}(1 + K_{\rm charge} \pm 2K_{\rm asy})\right], \\ dK_{\rm charge}/dl &= -4\tau_c^2\left[K_{\rm charge}\left(V_L^2 + V_R^2\right) + K_{\rm asy}\left(V_L^2 - V_R^2\right)\right], \\ dK_{\rm asy}/dl &= -2\tau_c^2\left[K_{\rm asy}\left(V_L^2 + V_R^2\right) + \left(V_L^2 - V_R^2\right)\right], \end{aligned} \quad (2)$$

where parameter l indicates the RG flow progress [44]: it equals zero at the beginning of RG, and increases when temperature T decreases $l \sim \ln(T_0/T)$, with T_0 the initial temperature (a device-dependent parameter that can only be characterized experimentally). $K_{\rm charge}$, with its initial value $1/(1+r)$, refers to the scaling dimension of the common field ϕ_c. $K_{\rm asy}$, which equals zero initially, refers to the scaling dimension from the left-right asymmetry [18,41]. These two parameters are introduced to model the change of bosonic-field correlation functions, during the RG flow. Briefly, these two parameters are introduced to model two influences of the RG flow. Firstly, during the RG flow, common field correlation, which equals $\langle \exp[i\phi_c(t)]\exp[-i\phi_c(0)]\rangle_{\rm initial} \propto 1/t$ initially, becomes modified into the effective correlation $\langle \exp[i\phi_c(t)]\exp[-i\phi_c(0)]\rangle_{\text{RG-effective}} \propto 1/t^{K_{\rm charge}}$. As the second effect, if $V_L \neq V_R$, the common (ϕ_c) and difference (ϕ_f) fields, which were initially uncorrelated, obtain the effective correlation $\langle \exp[i\phi_c(t)]\exp[-i\phi_f(0)]\rangle_{\text{RG-effective}} \propto 1/t^{K_{\rm asy}}$, leading to, crucially, different correlations of bosonic fields (ϕ_L and ϕ_R). Correlations above, evaluated during the RG flow, on the other hand, define these two quantities $K_{\rm charge}$ and $K_{\rm asy}$. Crucially, these two parameters are conventionally

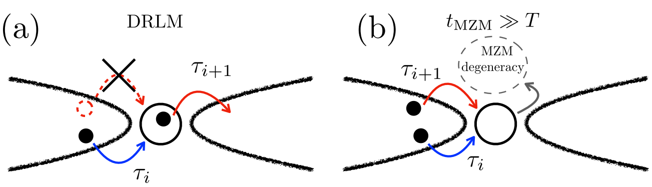

FIG. 3. Lead-impurity tunneling events. (a) In a regular DRLM, the dot state alternates (between two degenerate dot states) in time. (b) In great contrast, with tunneling into the MZM degeneracy (the gray arrow), two neighboring dot-lead tunneling events (shown by the blue and red arrows) can both contain a creation operator in the dot.

involved in studying interacting systems (e.g., Refs. [34,41]). For the symmetric case $V_L = V_R$, K_{asy} is fixed at zero [red dashed line of Fig. 2(c)]. The scaling dimension of lead-dot tunnelings becomes smaller than 1 (thus RG relevant) when K_{charge} has become smaller than $K_C = 4/(1+r) - 1$. For asymmetric situations, by contrast, $|K_{\mathrm{asy}}|$ increases during the RG flow [blue dashed line of Fig. 2(c)], after which the larger lead-dot coupling becomes more relevant than the weaker one, leading to an even more significant asymmetry [44]. The high-temperature flow terminates when $T \sim t_{\mathrm{M}}$.

Low-temperature RG and the phase diagram. For the low-temperature case $T \ll t_{\mathrm{M}}$, only ground states are allowed as real states in the impurity, and after one lead-dot tunneling, the impurity system prefers to evolve to one of the ground states ($|\psi_1\rangle$ or $|\psi_2\rangle$) before the next lead-dot tunneling event. Neighboring dot operators can be thus the same: a consequence of the presence of topological degeneracy. Low-temperature RG equations of an MZM-involved system become [44]

$$dV_{L,R}/dl = V_{L,R}\left[1 - \frac{1+r}{4}(1 + K_{\mathrm{charge}} \pm 2K_{\mathrm{asy}})\right],$$
$$dK_{\mathrm{charge}}/dl = 0, \quad dK_{\mathrm{asy}}/dl = -2\tau_c^2\left(V_L^2 + V_R^2\right)K_{\mathrm{asy}}, \quad (3)$$

with initial values of K_{charge} and K_{asy}, importantly, inherited from the RG-flow of the previous stage. The low-temperature flow Eq. (3) contains two major Majorana-induced modifications: (1) K_{charge}, which initially decreases in the high-temperature situation [solid lines of Fig. 2(c)], now stops flowing [solid lines of Fig. 2(d)], and, more importantly, (2) K_{asy}, which increases in the asymmetric case of the high-temperature limit [dashed red line of Fig. 2(c)], now instead begins to decrease to zero [dashed lines of Fig. 2(d)]. Modification (2), remarkably, is the key element that leads to the irrelevance of a weak asymmetry. Indeed, when K_{asy} has vanished, $dV_{L,R}/dl = V_{L,R}[1 - (1+r)(1 + K_{\mathrm{charge}})/4]$, where V_L and V_R simultaneously increase to perfect or decrease to zero, disregarding a weak asymmetry. Noticeably, the irrelevance of asymmetry also removes phases C and D in Fig. 1(c), where only one lead-impurity coupling (the smaller one of V_L or V_R) flows to zero. As the consequence of (1), the final phase is determined by the value of K_{charge}, larger or smaller than K_C, at the end of high-temperature flow [as shown in Fig. 2(d)].

One can physically understand these two modifications with Fig. 3. Briefly, in DRLM [with corresponding RG equations (2)] the dot state alternates in time [Fig. 3(a)], where $N_L + N_R$ has only two possible (integer) options. Field ϕ_c, reflecting fluctuations of $N_L + N_R$, then gradually loses its scaling dimension [reflected by the decreasing K_{charge} of Eq. (2)] when $N_L + N_R$ is fixed by a half-filling dot [41]. In great contrast, with Majorana involved, the parity of the impurity part, including the dot and a coupled MZM, alternates in time [Fig. 3(b)]. The corresponding common field ϕ_c now becomes a free 1D field. Its scaling dimension K_{charge} thus remains invariant during the RG flow of Eq. (3). We emphasize, importantly, the necessity of topological degeneracy in the picture above. Instead, if the DRLM dot couples to a zero-energy Andreev bound state (ABS), the case can reduce to the DRLM with a detuned dot [44]: a system with only the isolated-impurity phase [16–18]. This effective detuning is proportional to the difference in amplitudes of normal and Andreev tunnelings between ABS and the dot. Crucially, assuming the effective detuning ε (not the inter-MZM coupling that can be reduced by increasing the nanowire size), it obeys [44]

$$\frac{d}{dl}\varepsilon = \varepsilon + \frac{\tau_c\left(V_L^2 + V_R^2\right)}{4}\left(e^{-\varepsilon\tau_c} - e^{\varepsilon\tau_c}\right) \quad (4)$$

and grows during the RG flow. Consequently, however small initially, ε becomes dominant, driving the system to the zero-conductance phase at energies much smaller than ε. Specially, ε equals zero initially, for an accidentally fine-tuned ABS. It however will not provide an extended ballistic-transmission phase, due to inevitable cross-talks between tuning gates [44].

Modifications above also explain features of Figs. 2(a) and 2(b). More specifically, with a larger t_{M} of Fig. 2(a), (1) for the symmetric case, a larger value of $V_L = V_R$ is required to enter the ballistic-transmission phase, and (2) for the asymmetric case, the ballistic-transmission phase tolerates a larger value of $V_L - V_R$. Feature (1) is a consequence of an earlier termination, due to a larger t_{M}, of the high-temperature flow. Feature (2) is related to the nonmonotonous curve of K_{charge} [blue solid line of Fig. 2(c)].

Discussion. In this paper, we show that the MZM-introduced topological degeneracy can relax the strict symmetry requirement $V_L = V_R$ for a BKT QPT in a DRLM. This result can be understood with the g-theorem [31,32], by visiting the effect of a weak asymmetry in the strong tunneling regime. Briefly, the g-theorem claims that in a boundary QPT, the phase with a smaller degeneracy is more stable. Indeed, in a regular asymmetry-present DRLM, the fixed point where the dot is fully hybridized by the stronger lead has a smaller degeneracy [degeneracy $g = 1$, in Fig. 4(b)] than that of the ballistic-transmission fixed point [$g = \sqrt{1+r}$ [59], Fig. 4(a)]. The zero-conductance phase is thus more stable in a regular DRLM. With the Majorana provided, the fixed point where the dot is hybridized by the stronger lead has the degeneracy $\sqrt{2}$ [Fig. 4(d)], the degeneracy of a single MZM: larger than that [Fig. 4(b)] of the MZM absent situation. For the ballistic transmission case, the Majorana couples to the residued dot degeneracy (i.e., $\sqrt{1+r}$). The degeneracy of the impurity part, obtained after the MZM-residue fusion [60,61] (see Ref. [62], a pioneering example), is generally hard to obtain. Indeed, an arbitrary r does not necessarily correspond to a discrete Virasoro algebra with central charge $c < 1$ [60]. We can, however, evaluate the possible range of degeneracy, with fusion between primary

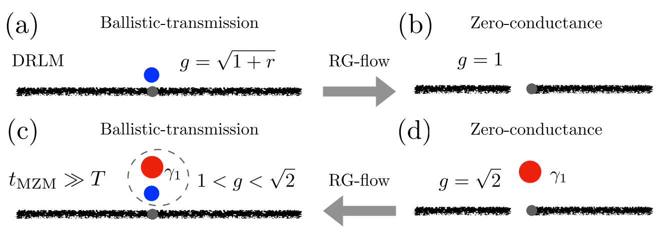

FIG. 4. The effect of left-right asymmetry (assuming $V_L < V_R$) in a regular (a and b) and Majorana-involved DRLM (c and d). The red and blue dots refer to the MZM and the residue degeneracy ($g = \sqrt{1+r}$) of the ballistic-transmission phase, respectively. The gray dot instead indicates the hybridized dot degree of freedom. RG flow prefers the fixed point with a smaller degeneracy.

fields of the Ising model ($c = 1/2$). Indeed, if $r = 1$, we have the fusion $[\sqrt{1+r}] \times [\sqrt{2}] = [\sqrt{2}] \times [\sqrt{2}] = [1] + [2]$, with numbers indicating the degeneracy. For $r = 3$, instead $[\sqrt{1+r}] \times [\sqrt{2}] = [2] \times [\sqrt{2}] = [\sqrt{2}] + [2\sqrt{2}]$. Taking the smaller degeneracy of both cases, the Majorana-involved ballistic-transmission phase thus has a smaller degeneracy [$1 < g < \sqrt{2}$, Fig. 4(c)] than that ($\sqrt{2}$) of the zero-conductance one, indicating a stabilized ballistic-transmission phase against a weak asymmetry. Importantly, similar g-theorem analysis applies to situations with a finite ϵ_d: the BKT QPT thus tolerates also a small dot detuning [44].

Before closure, we emphasize that the predicted modification of the BKT QPT phase diagram can further confirm a plausible Majorana signature (if any), through the detection of the nontrivial MZM degeneracy. Indeed, with a zero-energy ABS (which notoriously reduces the reliability of Majorana signals), the impurity part, including the resonant level and the ABS, is gapped in energy [i.e., ε of Eq. (4)], resulting in a suppressed current at low energies. A detailed calculation and corresponding g-theorem analysis are provided in the Supplemental Material [44]. Remarkably, conclusions above even remain applicable to situations where the hybrid nanowire has multiple conductance channels. Encouraged by persistent progress of Majorana hunting in nanodevices [63–72], especially for the cases with dissipative environments [73–77], we anticipate the experimental capability to introduce enough dissipation in potential Majorana-hosted candidates. Prospectively, other QPT-hosted systems (either one-dimensional ones or systems with multiple boundary QPTs) can potentially help the identification of Majorana nonlocalities [78–84], another crucial element in topological quantum devices.

Acknowledgments. The authors thank H. Zhang for valuable discussions. This work was supported by the Innovation Program for Quantum Science and Technology (Grant No. 2021ZD0302400) and the National Natural Science Foundation of China (Grants No. 11974198, No. 12374158, and No. 12074039).

[1] M. Vojta, Impurity quantum phase transitions, Philos. Mag. **86**, 1807 (2006).
[2] I. Affleck, Quantum impurity problems in condensed matter physics, arXiv:0809.3474.
[3] I. Affleck and A. W. W. Ludwig, Critical theory of overscreened Kondo fixed points, Nucl. Phys. B **360**, 641 (1991).
[4] I. Affleck, A. W. W. Ludwig, H.-B. Pang, and D. L. Cox, Relevance of anisotropy in the multichannel Kondo effect: Comparison of conformal field theory and numerical renormalization-group results, Phys. Rev. B **45**, 7918 (1992).
[5] V. J. Emery and S. Kivelson, Mapping of the two-channel Kondo problem to a resonant-level model, Phys. Rev. B **46**, 10812 (1992).
[6] A. K. Mitchell, L. A. Landau, L. Fritz, and E. Sela, Universality and scaling in a charge two-channel Kondo device, Phys. Rev. Lett. **116**, 157202 (2016).
[7] P. L. S. Lopes, I. Affleck, and E. Sela, Anyons in multichannel Kondo systems, Phys. Rev. B **101**, 085141 (2020).
[8] A. Komnik and A. O. Gogolin, Resonant tunneling between Luttinger liquids: A solvable case, Phys. Rev. Lett. **90**, 246403 (2003).
[9] B. A. Jones and C. M. Varma, Study of two magnetic impurities in a Fermi gas, Phys. Rev. Lett. **58**, 843 (1987).
[10] B. A. Jones, B. G. Kotliar, and A. J. Millis, Mean-field analysis of two antiferromagnetically coupled Anderson impurities, Phys. Rev. B **39**, 3415 (1989).
[11] I. Affleck and A. W. W. Ludwig, Exact critical theory of the two-impurity Kondo model, Phys. Rev. Lett. **68**, 1046 (1992).
[12] C. Sire, C. M. Varma, and H. R. Krishnamurthy, Theory of the non-Fermi-liquid transition point in the two-impurity Kondo model, Phys. Rev. B **48**, 13833 (1993).
[13] M. Garst, S. Kehrein, T. Pruschke, A. Rosch, and M. Vojta, Quantum phase transition of Ising-coupled Kondo impurities, Phys. Rev. B **69**, 214413 (2004).
[14] R. Žitko and J. Bonča, Multiple-impurity Anderson model for quantum dots coupled in parallel, Phys. Rev. B **74**, 045312 (2006).
[15] R. Žitko, J. Mravlje, and K. Haule, Ground state of the parallel double quantum dot system, Phys. Rev. Lett. **108**, 066602 (2012).
[16] H. T. Mebrahtu, I. V. Borzenets, D. E. Liu, H. Zheng, Yu. V. Bomze, A. I. Smirnov, H. U. Baranger, and G. Finkelstein, Quantum phase transition in a resonant level coupled to interacting leads, Nature (London) **488**, 61 (2012).
[17] H. T. Mebrahtu, I. V. Borzenets, H. Zheng, Yu. V. Bomze, A. I. Smirnov, S. Florens, H. U. Baranger, and G. Finkelstein, Observation of Majorana quantum critical behavior in a resonant level coupled to a dissipative environment, Nat. Phys. **9**, 732 (2013).
[18] D. E. Liu, H. Zheng, G. Finkelstein, and H. U. Baranger, Tunable quantum phase transitions in a resonant level coupled to two dissipative baths, Phys. Rev. B **89**, 085116 (2014).
[19] E. Cornfeld, L. A. Landau, K. Shtengel, and E. Sela, Entanglement spectroscopy of non-Abelian anyons: Reading off quantum dimensions of individual anyons, Phys. Rev. B **99**, 115429 (2019).
[20] Y. Komijani, Isolating Kondo anyons for topological quantum computation, Phys. Rev. B **101**, 235131 (2020).

[21] M. Lotem, E. Sela, and M. Goldstein, Manipulating non-Abelian anyons in a chiral multichannel Kondo model, Phys. Rev. Lett. **129**, 227703 (2022).
[22] D. Gabay, C. Han, P. L. S. Lopes, I. Affleck, and E. Sela, Multi-impurity chiral Kondo model: Correlation functions and Anyon fusion rules, Phys. Rev. B **105**, 035151 (2022).
[23] G. Zhang and C. Spånslätt, Distinguishing between topological and quasi Majorana zero modes with a dissipative resonant level, Phys. Rev. B **102**, 045111 (2020).
[24] C.-H. Chung, K. Le Hur, M. Vojta, and P. Wölfle, Nonequilibrium transport at a dissipative quantum phase transition, Phys. Rev. Lett. **102**, 216803 (2009).
[25] A. Yu. Kitaev, Unpaired Majorana fermions in quantum wires, Phys.-Usp. **44**, 131 (2001).
[26] R. M. Lutchyn, J. D. Sau, and S. Das Sarma, Majorana fermions and a topological phase transition in semiconductor-superconductor heterostructures, Phys. Rev. Lett. **105**, 077001 (2010).
[27] Y. Oreg, G. Refael, and F. von Oppen, Helical liquids and Majorana bound states in quantum wires, Phys. Rev. Lett. **105**, 177002 (2010).
[28] N. Read and D. Green, Paired states of fermions in two dimensions with breaking of parity and time-reversal symmetries and the fractional quantum Hall effect, Phys. Rev. B **61**, 10267 (2000).
[29] L. Fu and C. L. Kane, Superconducting proximity effect and Majorana fermions at the surface of a topological insulator, Phys. Rev. Lett. **100**, 096407 (2008).
[30] C. Nayak, S. H. Simon, A. Stern, M. Freedman, and S. Das Sarma, Non-Abelian anyons and topological quantum computation, Rev. Mod. Phys. **80**, 1083 (2008).
[31] I. Affleck and A. W. W. Ludwig, Universal noninteger "ground-state degeneracy" in critical quantum systems. Phys. Rev. Lett. **67**, 161 (1991).
[32] I. Affleck and A. W. W. Ludwig, Exact conformal-field-theory results on the multichannel Kondo effect: Single-fermion Green's function, self-energy, and resistivity, Phys. Rev. B **48**, 7297 (1993).
[33] D. Friedan and A. Konechny, Boundary entropy of one-dimensional quantum systems at low temperature, Phys. Rev. Lett. **93**, 030402 (2004).
[34] A. Schiller and K. Ingersent, Renormalization-group study of a magnetic impurity in a Luttinger liquid, Europhys. Lett. **39**, 645 (1997).
[35] G.-L. Ingold and Yu. V. Nazarov, Charge tunneling rates in ultrasmall junctions, in *Single Charge Tunneling: Coulomb Blockade Phenomena In Nanostructures*, edited by H. Grabert and M. H. Devoret (Springer US, Boston, 1992), pp. 21–107.
[36] F. D. Parmentier, A. Anthore, S. Jezouin, H. le Sueur, U. Gennser, A. Cavanna, D. Mailly, and F. Pierre, Strong back-action of a linear circuit on a single electronic quantum channel, Nat. Phys. **7**, 935 (2011).
[37] S. Jezouin, M. Albert, F. D. Parmentier, A. Anthore, U. Gennser, A. Cavanna, I. Safi, and F. Pierre, Tomonaga-Luttinger physics in electronic quantum circuits, Nat. Commun. **4**, 1802 (2013).
[38] Yu. V. Nazarov, Anomalous current-voltage characteristics of tunnel junctions, Zh. Eksp. Teor. Fiz. **95**, 975 (1989) [Sov. Phys. JETP **68**, 561 (1989)].
[39] I. Safi and H. Saleur, One-channel conductor in an Ohmic environment: Mapping to a Tomonaga-Luttinger liquid and full counting statistics, Phys. Rev. Lett. **93**, 126602 (2004).
[40] S. Florens, P. Simon, S. Andergassen, and D. Feinberg, Interplay of electromagnetic noise and Kondo effect in quantum dots, Phys. Rev. B **75**, 155321 (2007).
[41] C. L. Kane and M. P. A. Fisher, Transmission through barriers and resonant tunneling in an interacting one-dimensional electron gas, Phys. Rev. B **46**, 15233 (1992).
[42] T. Giamarchi, *Quantum Physics in One Dimension* (Oxford University, Oxford, 2004).
[43] The QPT is not of BKT type when $r < 2$ [16]. When $r > 3$, the dot is always isolated.
[44] See Supplemental Material at http://link.aps.org/supplemental/10.1103/PhysRevB.109.L161110 for (i) RG equations and descriptions of BKT QPT in a regular DRLM, (ii) correlation function of the impurity part, (iii) derivations of RG equations in the low-temperature regime, (iv) RG flow equations in the presence of a finite detuning of the dot (ϵ_d), (v) the situation that the DRLM dot couples to a topologically trivial Andreev bound state, and (vi) a proposed protocol, assisted by the BKT transition, to further strength the credibility of a plausible Majorana signal.
[45] D. E. Liu and H. U. Baranger, Detecting a Majorana-fermion zero mode using a quantum dot, Phys. Rev. B **84**, 201308(R) (2011).
[46] E. Vernek, P. H. Penteado, A. C. Seridonio, and J. C. Egues, Subtle leakage of a Majorana mode into a quantum dot, Phys. Rev. B **89**, 165314 (2014).
[47] I. Safi and H. J. Schulz, Transport in an inhomogeneous interacting one-dimensional system, Phys. Rev. B **52**, R17040 (1995).
[48] D. L. Maslov and M. Stone, Landauer conductance of Luttinger liquids with leads, Phys. Rev. B **52**, R5539 (1995).
[49] V. V. Ponomarenko, Renormalization of the one-dimensional conductance in the Luttinger-liquid model, Phys. Rev. B **52**, R8666 (1995).
[50] A. Kawabata, On the renormalization of conductance in Tomonaga-Luttinger liquid, J. Phys. Soc. Jpn. **65**, 30 (1996).
[51] C. C. Chamon and E. Fradkin, Distinct universal conductances in tunneling to quantum Hall states: The role of contacts, Phys. Rev. B **56**, 2012 (1997).
[52] Y. Hu and C. L. Kane, Universal symmetry-protected resonances in a spinful Luttinger liquid, arXiv:1604.08280.
[53] V. L. Berezinskii, Destruction of long-range order in one-dimensional and two-dimensional systems having a continuous symmetry group I. Classical systems, Zh. Eksp. Teor. Fiz. **59**, 907 (1971) [Sov. Phys. JETP **32**, 493 (1971)].
[54] J. M. Kosterlitz, The critical properties of the two-dimensional XY model, J. Phys. C **7**, 1046 (1974).
[55] J. M. Kosterlitz and D. J. Thouless, Ordering, metastability and phase transitions in two-dimensional systems, in *Basic Notions Of Condensed Matter Physics* (CRC Press, Boca Raton, 2018), pp. 493–515.
[56] A. Altland and B. D. Simons, *Condensed Matter Field Theory*, 2nd ed. (Cambridge University, Cambridge, 2010).
[57] P. W. Anderson, G. Yuval, and D. R. Hamann, Exact results in the Kondo problem. II. Scaling theory, qualitatively correct solution, and some new results on one-dimensional classical statistical models, Phys. Rev. B **1**, 4464 (1970).

[58] H. Bruus and K. Flensberg, *Many-Body Quantum Theory in Condensed Matter Physics – An Introduction* (Oxford University, New York, 2004).
[59] H. Zheng, S. Florens, and H. U. Baranger, Transport signatures of Majorana quantum criticality realized by dissipative resonant tunneling, Phys. Rev. B **89**, 235135 (2014).
[60] P. Ginsparg, Fields, *Strings and Critical Phenomena (Les Houches, Session XLIX, 1988)*, edited by E. Brézin and J. Zinn Justin (North-Holland, Amsterdam, 1989).
[61] P. D. Francesco, P. Mathieu, and D. Sénéchal, *Condensed Matter Field Theory*, 1st ed. (Springer, New York, 1997).
[62] I. Affleck, A. W. W. Ludwig, and B. A. Jones, Conformal-field-theory approach to the two-impurity Kondo problem: Comparison with numerical renormalization-group results, Phys. Rev. B **52**, 9528 (1995).
[63] V. Mourik, K. Zuo, S. M. Frolov, S. R. Plissard, E. P. A. M. Bakkers, and L. P. Kouwenhoven, Signatures of Majorana fermions in hybrid superconductor-semiconductor nanowire devices, Science **336**, 1003 (2012).
[64] M. T. Deng, S. Vaitiekėnas, E. B. Hansen, J. Danon, M. Leijnse, K. Flensberg, J. Nygård, P. Krogstrup, and C. M. Marcus, Majorana bound state in a coupled quantum-dot hybrid-nanowire system, Science **354**, 1557 (2016).
[65] S. M. Albrecht, A. P. Higginbotham, M. Madsen, F. Kuemmeth, T. S. Jespersen, J. Nygård, P. Krogstrup, and C. M. Marcus, Exponential protection of zero modes in Majorana islands, Nature (London) **531**, 206 (2016).
[66] A. Fornieri, A. M. Whiticar, F. Setiawan, E. Portolés, A. C. Drachmann, A. Keselman, S. Gronin, C. Thomas, T. Wang, R. Kallaher *et al.*, Evidence of topological superconductivity in planar Josephson junctions, Nature (London) **569**, 89 (2019).
[67] H. Ren, F. Pientka, S. Hart, A. T. Pierce, M. Kosowsky, L. Lunczer, R. Schlereth, B. Scharf, E. M. Hankiewicz, L. W. Molenkamp *et al.*, Topological superconductivity in a phase-controlled Josephson junction, Nature (London) **569**, 93 (2019).
[68] S. Vaitiekėnas, Y. Liu, P. Krogstrup, and C. Marcus, Zero-bias peaks at zero magnetic field in ferromagnetic hybrid nanowires, Nat. Phys. **17**, 43 (2021).
[69] H. Song, Z. Zhang, D. Pan, D. Liu, Z. Wang, Z. Cao, L. Liu, L. Wen, D. Liao, R. Zhuo, D. E. Liu, R. Shang, J. Zhao, and H. Zhang, Large zero bias peaks and dips in a four-terminal thin InAs-Al nanowire device, Phys. Rev. Res. **4**, 033235 (2022).
[70] Z. Wang, H. Song, D. Pan, Z. Zhang, W. Miao, R. Li, Z. Cao, G. Zhang, L. Liu, L. Wen, R. Zhuo, D. E. Liu, K. He, R. Shang, J. Zhao, and H. Zhang, Plateau regions for zero-bias peaks within 5% of the quantized conductance value $2e^2/h$, Phys. Rev. Lett. **129**, 167702 (2022).
[71] M. Aghaee, A. Akkala, Z. Alam, R. Ali, A. A. Ramirez, M. Andrzejczuk, A. E. Antipov, M. Astafev, B. Bauer, J. Becker *et al.*, InAs-Al hybrid devices passing the topological gap protocol, Phys. Rev. B **107**, 245423 (2023).
[72] T. Dvir, G. Wang, N. van Loo, C.-X. Liu, G. P. Mazur, A. Bordin, S. L. D. ten Haaf, J.-Y. Wang, D. van Driel, F. Zatelli, X. Li, F. K. Malinowski, S. Gazibegovic, G. Badawy, E. P. A. M. Bakkers, M. Wimmer, and L. P. Kouwenhoven, Realization of a minimal Kitaev chain in coupled quantum dots, Nature (London) **614**, 445 (2023).
[73] D. E. Liu, Proposed method for tunneling spectroscopy with ohmic dissipation using resistive electrodes: A possible Majorana filter, Phys. Rev. Lett. **111**, 207003 (2013).
[74] D. Liu, G. Zhang, Z. Cao, H. Zhang, and D. E. Liu, Universal conductance scaling of Andreev reflections using a dissipative probe, Phys. Rev. Lett. **128**, 076802 (2022).
[75] S. Zhang, Z. Wang, D. Pan, H. Li, S. Lu, Z. Li, G. Zhang, D. Liu, Z. Cao, L. Liu, L. Wen, D. Liao, R. Zhuo, R. Shang, D. E. Liu, J. Zhao, and H. Zhang, Suppressing Andreev bound state zero bias peaks using a strongly dissipative lead, Phys. Rev. Lett. **128**, 076803 (2022).
[76] Z. Wang, S. Zhang, D. Pan, G. Zhang, Z. Xia, Z. Li, D. Liu, Z. Cao, L. Liu, L. Wen, D. Liao, R. Zhuo, Y. Li, D. E. Liu, R. Shang, J. Zhao, and H. Zhang, Large Andreev bound state zero-bias peaks in a weakly dissipative environment, Phys. Rev. B **106**, 205421 (2022).
[77] S. Zhang, Z. Wang, D. Pan, Z. Wang, Z. Li, Z. Zhang, Y. Gao, Z. Cao, G. Zhang, L. Liu *et al.*, *In situ* tuning of dynamical Coulomb blockade on Andreev bound states in hybrid nanowire devices, Phys. Rev. B **108**, 235416 (2023).
[78] G. W. Semenoff and P. Sodano, Teleportation by a Majorana medium, arXiv:cond-mat/0601261.
[79] L. Fu, Electron teleportation via Majorana bound states in a mesoscopic superconductor, Phys. Rev. Lett. **104**, 056402 (2010).
[80] B. Béri and N. R. Cooper, Topological Kondo effect with Majorana fermions, Phys. Rev. Lett. **109**, 156803 (2012).
[81] A. Altland and R. Egger, Multiterminal Coulomb-Majorana junction, Phys. Rev. Lett. **110**, 196401 (2013).
[82] B. Béri, Majorana-Klein hybridization in topological superconductor junctions, Phys. Rev. Lett. **110**, 216803 (2013).
[83] A. Altland, B. Béri, R. Egger, and A. M. Tsvelik, Multichannel Kondo impurity dynamics in a Majorana device, Phys. Rev. Lett. **113**, 076401 (2014).
[84] Y. Hao, G. Zhang, D. Liu, and D. E. Liu, Anomalous universal conductance as a hallmark of non-locality in a Majorana-hosted superconducting island, Nat. Commun. **13**, 6699 (2022).